

Nanocrystallization in $\text{Co}_{67}\text{Cr}_7\text{Fe}_4\text{Si}_8\text{B}_{14}$ Amorphous Alloy Ribbons

Z. Jamili-Shirvan¹, M. Haddad-Sabzevar¹

Abstract

The nanocrystallization of $\text{Co}_{67}\text{Fe}_4\text{Cr}_7\text{Si}_8\text{B}_{14}$ amorphous ribbons which prepared by planar flow melt spinning process (PFMS) was investigated. Crystallization of the ribbons was studied by differential thermal analysis (DTA), X-ray diffraction (XRD) and transmission electron microscopy (TEM). The DTA result of amorphous ribbon at heating rate of $10^\circ\text{C}/\text{min}$ showed occurrence of phase transitions in two stages. The ribbons were isothermally annealed for 30 minutes in argon atmosphere at different temperatures between 300 and 650°C with 25°C steps. The magnetic properties of annealed samples were measured using a vibrating sample magnetometer (VSM). The VSM results revealed that optimum soft magnetic properties occurred at 400°C . XRD patterns showed that the samples isothermally annealed up to 450°C were amorphous, while TEM results at 400°C indicated 7-8 nm mean size nanocrystallites in amorphous matrix and size of the nanocrystallites increased by increasing temperature. Also by X-ray diffraction pattern, precipitation of different phases at higher temperatures confirmed.

Keywords: Amorphous Alloy; Transmission Electron Microscopy; Nanocrystallization, Soft Magnetic Properties; XRD

1. Introduction

Amorphous alloys can be prepared by various techniques, such as melt spinning, mechanical alloying, vapor deposition, chemical alloying, etc. [1].

The rapid solidification of metallic alloys by melt spinning technique can produce amorphous or nanocrystalline materials.

Metallic glasses can crystallize when heated or held at elevated temperatures for sufficient time. Crystallization occurs with some changes in properties, such as heat capacity and electrical resistivity and magnetic properties. The crystallization behavior of metallic glasses has been studied by many researchers [2-5]. It has been reported that either the magnetic properties may deteriorate after crystallization, or they may be improved if nanocrystalline phases formed [1]. The anisotropy reduction combines with the near-zero magnetostriction, associated with the two-phase nature of the sample (nanocrystalline phase in amorphous matrix), to produce excellent soft magnetic properties [6].

The Co-rich amorphous alloy has attracted great interest for a variety of applications

including electronics, magnetic recordings and magnetic sensors due to its near-zero magnetostriction behavior [7-9] and giant magnetoimpedance (GMI) effect [10].

Recently, the hysteretic properties and saturation magnetostriction are reported for these nanocrystalline and amorphous Co-base alloys [11].

The nanocrystallization of Co-based metallic glasses is scarcely studied while substantial amount of work exists on those of Fe-based metallic glasses.

It is found that amorphous ribbon with composition of $\text{Co}_{67}\text{Fe}_4\text{Cr}_7\text{Si}_8\text{B}_{14}$ has the maximum GMI ratio [12] and an ultra-soft magnetic character because of the nearly zero magnetostriction value of the order of 1×10^{-7} [13-14]. In this work, the nanocrystallization of $\text{Co}_{67}\text{Fe}_4\text{Cr}_7\text{Si}_8\text{B}_{14}$ amorphous ribbon produced by planar flow melt spinning (PFMS) was studied.

2. Experimental Method

$\text{Co}_{67}\text{Fe}_4\text{Cr}_7\text{Si}_8\text{B}_{14}$ alloy used in this study was prepared from pure materials and melted in a vacuum furnace. The planar flow melt spinning (PFMS) process was used for

1- Department of Materials Engineering and Metallurgy, Faculty of Engineering, Ferdowsi University of Mashhad, Iran.

producing continuous ribbons. The samples were remelted in an induction furnace, using a quartz tube (as a crucible) with an inner diameter of about 20 mm under argon atmosphere. The crucible had a rectangular nozzle, by dimensions of 0.4×20 mm. The distance between the wheel and the nozzle was about 0.25-0.35 mm. A Pt- Pt-10%Rh thermocouple was positioned inside the melt to control the temperature. The melt was ejected by blowing argon at different casting temperatures. The continuous ribbons of about 20 mm width were produced, using a copper wheel (290 mm in diameter) as a substrate.

The amorphous ribbons were 29 ± 1 μm in thickness. The amorphous structure of the ribbon was confirmed by X-ray diffraction.

The thermal stability of the amorphous ribbon was investigated by differential thermal analyzer (NETZSCH 404) (DTA). The measurement was performed on 0.2 gr weight of the sample using $10^\circ\text{C}/\text{min}$ heating rate from room temperature to 1000 K in argon atmosphere.

The magnetic hysteresis loops of the as-prepared and heat treated samples were obtained by a vibrating sample magnetometer (VSM) at room temperature. Samples for this test were punched as discs with 3 mm diameter, then isothermally annealed in argon atmosphere for 30 minutes at temperature range $300\text{-}650^\circ\text{C}$ with 25°C steps.

X-ray diffraction (XRD) measurements (BRUKER axs, Model) were performed on heat treated ribbons. The XRD patterns were taken with the $\text{Cu-K}\alpha$ radiation, using 0.03° step increments for 2θ ($2\theta = 4\text{-}120^\circ$). Bright field images and electron diffraction patterns were observed using Transmission Electron Microscopy (TEM) for samples with optimal magnetic properties (heat treated at 400°C) and the samples heat treated at 450°C . The samples prepared for TEM observations were punched as 3mm discs and jet polished after heat treatment.

3. Result and Discussion

The crystallization behavior of the amorphous alloy is indicated in figure 1. The

crystallization of the $\text{Co}_{67}\text{Cr}_7\text{Fe}_4\text{Si}_8\text{B}_{14}$ amorphous alloy occurs in two stages. The onset temperatures of crystallization steps in the DTA curve at heating rate of $10^\circ\text{C}/\text{min}$ are 485°C and 585°C , respectively.

There are three types of crystallization transformation for amorphous alloys: primary, polymorphous and eutectic [1, 8, 15-16]. Koster et al. [17] experimentally demonstrated that the metallic glasses with primary crystallization are the most suitable candidates for nanocrystallization. Since there are two exothermic peaks in continues heating curve (Figure 1), thus crystallization of $\text{Co}_{67}\text{Fe}_4\text{Cr}_7\text{Si}_8\text{B}_{14}$ amorphous alloy is a primary type.

There are several reports about nanocrystallization of Fe-based and Co-based amorphous alloys and effect of incomplete nanocrystallization on improvement of soft magnetic properties such as increasing of saturation magnetization (M_s) and coercivity (H_c) reduction. In the present alloy, by isothermal heating at $300\text{-}400^\circ\text{C}$, increasing in saturation magnetization and reducing in coercivity took placed in comparison with as-prepared sample (Figure 2). According to this figure, maximum saturation magnetization (67 emu/g) and minimum coercivity (0.0491 Oe) are happened in sample which annealed at 400°C , whereas M_s and H_c for as-prepared sample are about 59 emu/g and 1.3869 Oe, respectively. However, above this temperature (e.g. $400\text{-}500^\circ\text{C}$) deterioration of soft magnetic properties is observed.

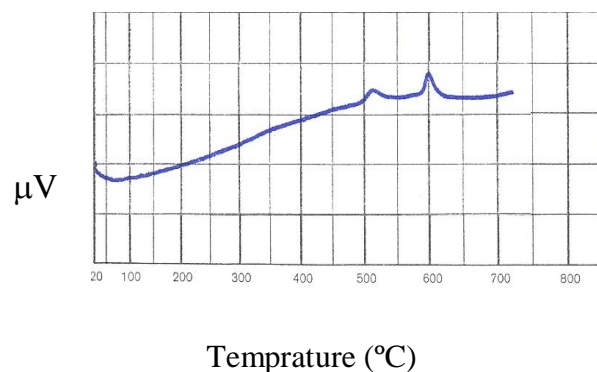


Fig. 1. DTA curve for amorphous $\text{Co}_{67}\text{Fe}_4\text{Cr}_7\text{Si}_8\text{B}_{14}$ alloy at heating rate of $10^\circ\text{C}/\text{min}$.

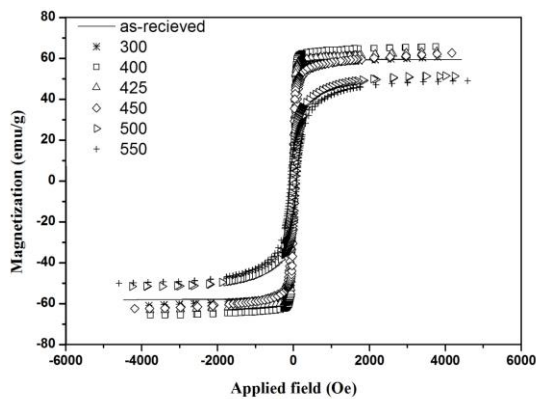


Fig. 2. Hysteresis loop of specimens isothermally annealed 30 minutes at different temperatures.

Formation of crystalline phases at different temperatures were investigated by X-ray diffraction. In the XRD spectra of the samples which annealed at 300-450 °C, any crystalline phases could not be identified by standard software. As an example, figure 3a shows XRD pattern of sample annealed at 450 °C.

Since the samples that isothermally annealed at 400°C had the best soft magnetic properties, these samples were studied by TEM. As illustrates in Figure 4.a the nanocrystallites with about 7-8 nm in size had distributed in an amorphous matrix. Electron diffraction pattern of this sample has exhibited in Figure 4.b. and was showed that the crystalline phases are very small in size.

The random distribution of the magnetization orientations in nanocrystallites and their dimensions below the exchange correlation length reduced the average crystalline anisotropy that is favorable for softening of the magnetic properties [5-6, 18].

According to Byumetal and Bordin et al. [11] and Byun et al. [7] reports, these nanocrystalline phases can be HCP-Co and Co_3B . These crystalline phases reveal in XRD pattern of annealed samples at 500°C (Figure 3.b). Bright field image of the specimen annealed at 450°C (the temperature that deterioration of soft magnetic properties was observed) was demonstrated in Figure 4.c.

According to this figure, increasing in annealing temperature from 400°C to 450°C

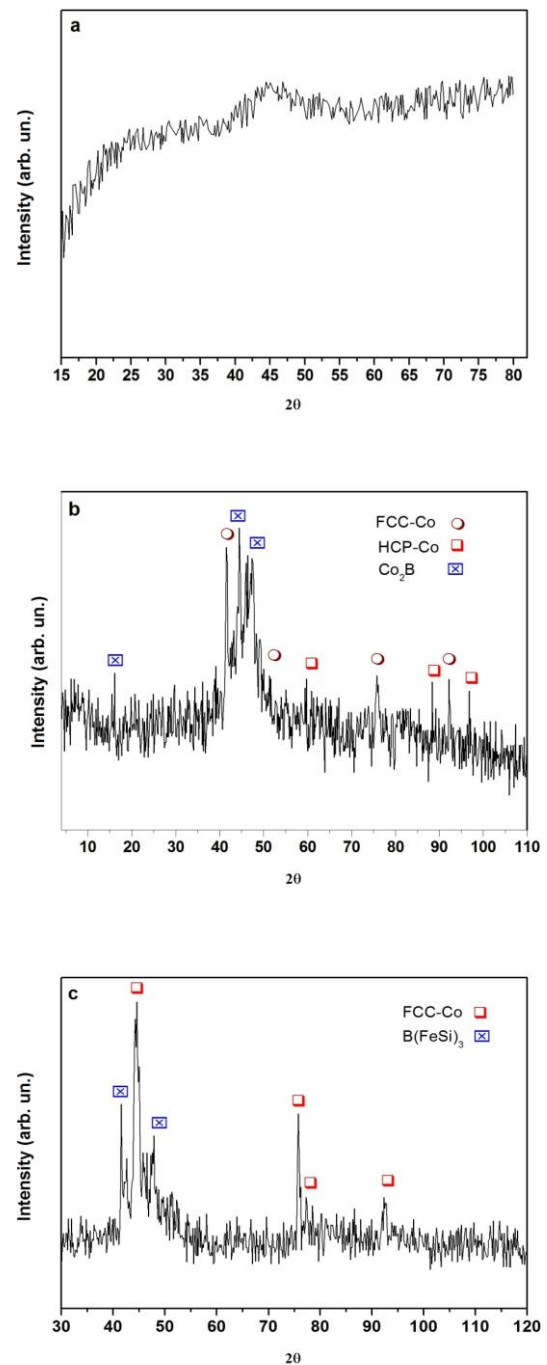


Fig. 3. X-ray diffraction patterns of $\text{Co}_{67}\text{Fe}_4\text{Cr}_7\text{Si}_8\text{B}_{14}$ amorphous alloy. Specimens were isothermally annealed 30 minutes at different temperatures, a) 450 b) 500°C, c) 550 °C.

significantly affected the crystallites growth. Thus, the main factor at this temperature for deterioration of soft magnetic properties (increase hysteresis loss, increase H_c and decrease M_s) is increasing of nanocrystallites

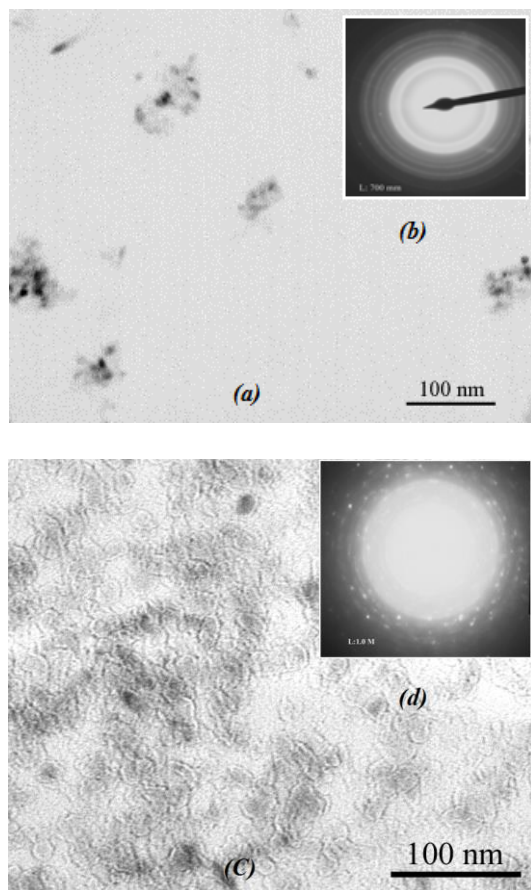


Fig. 4. TEM bright field image of sample was annealed at 400 °C (a).

Electron diffraction pattern of sample was annealed at 400 °C (b).

TEM bright field image of sample was annealed at 450 °C (c).

Electron diffraction pattern of sample was annealed at 450 °C (d) for 30 minutes.

dimension. Electron diffraction pattern of this sample (Figure 4.d) illustrates rings which form by discrete spots in luminous background. The spots usually suggest large grains included in the selected area diffraction (SAD) aperture.

Crystallization kinetics of $\text{Co}_{67}\text{Fe}_4\text{Cr}_7\text{Si}_8\text{B}_{14}$ amorphous alloy reported elsewhere [19]. The Avrami exponent was about one, therefore the nucleation site saturation was offered for crystallization of this alloy at 400 °C. It is evident that by increasing in annealing temperature up to 450°C grain growth happened.

The metallurgical background for nanocrystallization of present alloy can be related to pre-clusters nature that formed during rapid solidification. Nature of pre-

clusters depends on alloy composition. By comparison with the similar alloys [4, 7-8, 10], it can be said, boride clusters have $\text{Co}_x\text{B}_n\text{Si}_m$ compositions that x is lower and m , n are higher than the average concentration of the elements in the amorphous phase. The dimension of the clusters is very small and about some tens of atoms [20]. Suggestion of Si as cluster former is because of the highest tendency to combination with boron elements among other additives (Cr, Fe). Formation of boride like clusters results the local reduction of boron atoms in surrounded matrix, so chemical bonding between Co and B weakens. Therefore, boron rejection or outward diffusion of boron occurs at lower temperatures. After this, the remaining Co atoms become unstable (mixing enthalpy between two elements is negative) and the unit-cell of HCP-Co forms and finally Co_3B produces [21]. As a result, boride clusters have an important role in formation of nanocrystalline phases. Clusters provide the local chemical potential of the components to overcome the surface energy term in formation of the crystalline embryo with the critical concentrations and the dimensions [20].

Kisid and Lovas [20] did comprehensive research about additives effect on cluster formation. According to their results narrowing of second crystallization step and presence of $\text{B}(\text{FeSi})_3$ in samples annealed at 550 °C (Figure. 3c) confirm the authors assumption on boride clusters formation. According to the following reasons, Cr atoms control growth rate of crystallites as below:

1. Cr atoms have greatest radius among other additives in this composition and act as obstacles to boron and other elements diffusion.
2. As mentioned for the present alloy, transformation starts at low temperatures and crystallization is an ordering phenomenon that all of atoms must be participate in it, but Cr atoms have low diffusion coefficient at low temperatures [7] so does not take part in crystal coarsening.

Therefore, the Cr content is the most effective factor for controlling of the nanocrystallization process. The aim of

nanocrystallization in similar alloys is to obtain the best soft magnetic properties. Cr addition to Co-base amorphous alloys helps approaching of magnetostriction to zero [8] but reduces the saturation magnetization at the result of its anti-ferromagnetic property [7]. It is suggested that boron and silicon contents in alloy should be controlled to attain high volume fraction of clusters in amorphous matrix. At this condition, boron atoms which are trapped in boride clusters are increased, so at low temperatures nuclei have a problem to coarsen (low diffusion coefficient) and crystalline phases remain nano size.

4. Conclusions

-Crystallization of $\text{Co}_{67}\text{Cr}_7\text{Fe}_4\text{Si}_8\text{B}_{14}$ amorphous alloy occurred at two stages. Therefore, alloy is a suitable candidate for nanocrystallization.

-Optimum soft magnetic properties (low coercivity hysteresis, low loss and high saturation magnetization) observed in samples that isothermally annealed for 30 minutes at 400 °C.

-Microstructure of samples isothermally annealed at 400 °C included 7-8 nm size nanocrystalline phases in an amorphous matrix.

-Deterioration of soft magnetic properties above 400 °C (temperature with optimum soft magnetic properties) was attributed to increase of nanocrystallites dimension.

- It is suggested that boron and silicon content in alloy should be controlled to attain high volume fraction of nanocrystallites in amorphous matrix to improve soft magnetic properties at low temperatures.

Acknowledgement

The authors would like to thank Ferdowsi University of Mashhad and the Iran Nanotechnology Initiative Council for financial support.

References

1. Lesz, S., Nowosielski, R., Zajdel, A., Kostrubiec, B., Stoklosa, Z., *Arch. Sci. Eng.*, Vol. 28 (2007) pp. 91-97.

2. Greer, A. L., *Acta Metall.*, Vol. 30 (1982) pp. 171-192.
3. Morris, D. G., *Acta Metall.*, Vol. 29 (1981) pp. 1213-1220.
4. Botta, W. J., Negri, D., Yavari, A. R., *Non-cryst. Sol.*, Vol. 247 (1999) pp. 19-25.
5. Li, H. F., Ramanujan, R. V., *Mater. Sci. Eng. A*, Vol. 375-377 (2004) pp.1087-1091.
6. Saiseng, S., Winotai, P., Nilpairuch, S., Limsuwan, P., Tang, I. M., *Magn. Magn. Mater.*, Vol. 278 (2004) pp. 172-178.
7. Byun, T. Y., Oh, Y., Yoon, C. S., Kim, C. K., *Alloys Comps.*, Vol. 368 (2004) pp. 283-286.
8. Rho, I. C., Yoon, C. S., Kim, C. K., Byun, T.Y., Hon, K. S., *Mater. Sci. Eng.*, Vol. B96 (2002) pp. 48-52.
9. Yuan, Z. Z., Chen, X. D., Wang, B. X., Chen, Z. J., *Alloys Comps.*, Vol. 399 (2005) pp. 166-172.
10. Minic, D. M., Maricic, A. M., Dimitrijevic, R. Z., Ristic, M. M., *Alloys. Comps.*, Vol. 430 (2007) pp. 241-245.
11. Bordin, G., Buttino, G., Cecchetti, A., Poppi, M., *Magn. Magn. Mater.*, Vol. 195 (1999) pp. 583-587.
12. Kumari, S., Chatteraj, I., Panda, A. K., Mitra, A., Pal, S. K., *Phys. D: Appl. Phys.*, (2001) pp. 39-45.
13. Kraus, L., Pirota, K. R., Torrejón, J., Vázquez, M., *Non-Crys. Sol.*, Vol. 353 (2007) pp. 763-267.
14. Kraus, L., Fendrych, F., Švec, P., Bydžovský, J., Kollár, M., *optoelec. Advanced mater.*, Vol. 4 (2002) pp. 237-243.
15. Yoon, C. S., Lim, S. K., Yoon, C. S., Kim, C. K., *Alloys. Comps.*, Vol. 359 (2003) pp. 261-266.
16. Beelnaska, L., Kotur, B., Murdy, S., Kovbuz, M., Haneczok, G., Karolus, M., *Phys.*, Vol. 98 (2008) pp. 062010.
17. Koster, U., Schunemann, U., Blank-Bewersdorff, M., Brauer, S., Sutton, M., Stephenson, G. B., *Mater. Sci. Eng. A*, Vol. 133 (1991) pp. 611-615.
18. Hoque, S. M., Khan, F. A., Hakim, M. A., *Mater. Let.*, 61 (2007) pp. 1227-1230.
19. Haddad-sabzevar, M., Sahebian, S., Jamili, Z., Hasheminezhad, S. A., *Defect and Diffus. Forum*, Vol. 297-301 (2010) pp. 330-337.
20. Kisid-koszo, E., Lovas, A., *key eng. Matter.*, Vol. 81 (1993) pp. 209-214.
21. Ajmal, M., Khan, M. S., Shamim, A., *Solid State Chemist.*, Vol. 154 (2000) pp. 145-147.